

LOW ENERGY BEAM DIAGNOSTIC FOR APEX, THE LBNL VHF PHOTO-INJECTOR*

D. Filippetto[†], J. Byrd, M. Chin, C. Cork, S. De Santis, J. Feng, W.E. Norum, L. Doolittle, C. Papadopoulos, G. Portmann, D.G. Quintas, F. Sannibale, M. Stuart, R. Wells, M. Zolotorev
LBNL, Berkeley, CA 94720, U.S.A.

Abstract

A high-repetition rate (MHz-class), high-brightness electron beam photo-gun is under construction at Lawrence Berkeley National Laboratory in the framework of the Advanced Photo-injector EXperiment (APEX). The injector gun is based on a normal conducting 187 MHz RF cavity operating in CW mode. In its first operational phase it will deliver short bunches (~ 1 to tens of picoseconds) with energy of 750 keV, and bunch charges ranging from 1 pC to 1 nC. Different high efficiency cathode materials will be tested, and the beam quality will be studied as a function of parameters as charge, initial bunch length and transverse size, focusing strength. Both the laser and electron beam diagnostics have been designed to assure the needed flexibility. In particular a high-resolution electron diagnostic section after the photo-gun provides the necessary dynamic range for scanned beam parameters: energy and energy spread, charge and current, transverse and longitudinal phase spaces, slice properties. The photo-gun electron beam diagnostic layout is presented, and the hardware choices, resolution and achievable dynamical ranges are also discussed.

OVERVIEW

The electron beam parameter range for APEX are reported in Table 1. The project has been conceived as an R&D experiment on MHz-class photo-injectors, with an eye on the future possible application as driver of FEL light sources [1]. A normal conducting gun running in CW at 187 MHz has been specifically designed and constructed for this purpose [2]. The low frequency and the proper design make it compatible with very low vacuum levels (10^{-12} Torr) and with a load lock system. Such environment gives us the chance of testing in RF fields different cathode materials with high quantum efficiencies and poor lifetimes. An Ytterbium-doped fiber laser system has been designed by Lawrence Livermore National Laboratory. It provides 500 nJ pulses at 1 MHz (0.5 W) for second and fourth harmonic generation. Both 266 and 532 nm beams are delivered to the cathode, for different work function materials. Transverse and longitudinal pulse shaping will allow for different electron beam densities and aspect ratios.

The wide foreseen measurable beam parameter space make of the diagnostic a challenging issue. This is partially

*Work supported by the Director of the Office of Science of the US Department of Energy under Contract no. DE-AC02-05CH11231

[†]dfilippetto@lbl.gov

mitigated by the high repetition rate. Integrated measurements indeed may enhance the signal-to-noise ratio and increase the overall dynamic range. On the other hand, single-bunch measurements are essential for the estimation of jitters.

Table 1: APEX Beam Parameters

Parameter	Value	dimensions
Energy	750	keV
Charge	1-1000	pC
average current	$1\text{-}10^6$	nA
Emittance (rms)	<1	μm
repetition rate	$1\text{-}10^6$	Hz
Bunch length(rms)	1-30	ps

DIAGNOSTIC BEAMLIN

Full photo-injector characterization entails a deep understanding of the functional dependency of the beam quality out of the RF gun from all the variables listed above. The optimization of projected and slice beam parameters in transverse and longitudinal planes at low energies is indeed a central task for such machines, and determines the overall performances.

The layout of the first phase of APEX beamline is shown in Fig.1. Two solenoids along the line will keep the beam focused. Three beam position monitors and six magnetic correctors will monitor and control the orbit.

Thermal emittance and beam alignment on the cathode will be measured at the first screen, 1.5 m downstream the cathode plug. Solenoid beam based alignment will be also carried out relating beam centroid trajectories to the focussing strength.

A second solenoid after the screen ($z_{cathode} \sim 170$ cm) will be used to tune beam dimension at the first slit of the emittance measurement system. The transverse emittance will be measured for the full range of beam charges by using a double slit system and an insertable Faraday cup (FC), based on the Cornell design [3]. A quadrupole triplet match the beam Twiss parameters for the subsequent longitudinal and slice emittance measurements, performed by a 1.3 GHz single cell deflecting cavity (RFD) [4] and a dispersive section. Two imaging screens and two beam dumps complete the beamline.

The repetition rate is a major concern when designing the beam diagnostic. Deposited charge and energy may become critical and damage the diagnostic, cooling rates may become unfeasible. On the other side flexibility in the high

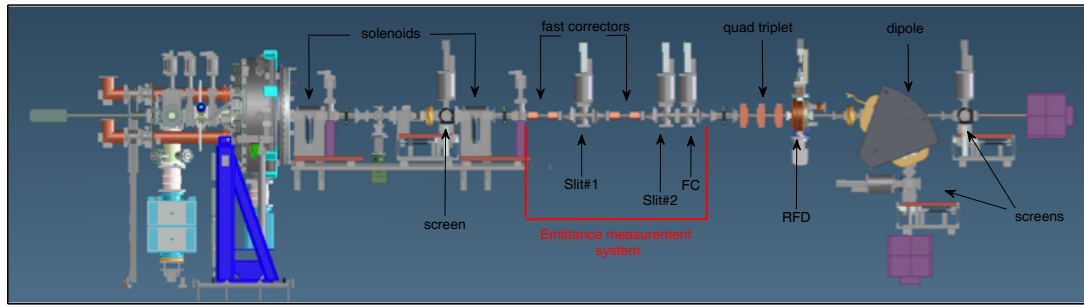


Figure 1: APEX layout for phase 1.

repetition rate can improve the signal-to-noise ratio (SNR) and may increase the overall dynamic range of diagnostic tools. In the case of intercepting screens for example, very low beam charge can be detected increasing the repetition rate, i.e. without changing the integrated signal in one readout cycle (\sim ms) on the CCD and avoiding screen saturation.

The thermal emittance is a key measurement in the determination of cathode performances. Also in this case the high repetition rate, together with the expected low dark current from such RF gun ($V_{rf}^{max} \sim 24$ MV), would consistently ease the measurement.

Charge, Current and Position Measurements

A complete source characterization implies both the measurement of beam parameters and their jitter around those values. As already said, a high repetition rate machine can take advantage of its average current, especially at very low charges. A femto-coulomb charge is indeed hardly detectable, while the 1 nA current produced at 1 MHz repetition rate is more easily measurable. Nevertheless an estimation of beam jitters requires bunch per bunch diagnostics, so for a full characterization both charge and current need to be measured. The range of charge and currents foreseen are summarized in Table 1. The machine won't normally operate with charges below 1 pC, but lower values may be present in particular cases as low QE cathode tests or beam scraping for measurements. The charge will be measured in different ways, depending on the needed sensitivity: one Beam Charge Monitor (BCM) will be placed before the first screen at ~ 1.3 m. Its dedicated electronics ([5]) can detect single bunch charges in the 1 nC-10 pC range at ~ 1 KHz. Low single bunch charges in the fC range will be measured with a chain of charge sensitive amplifier, a Gaussian shaping amplifier, and high speed digitizer connected to the FC signal [6]. A VME QDC module, with 25 fC minimum sensitivity, can also be used at bunch rates up to 100 KHz [7] with the FC.

For very low charges a current measurement would be more reliable. The beam current information will be measured at the Faraday Cup using a high resolution picoammeter [8]. The instrument can be configured for 1 nA full

scale measurements with 10 fA resolution at ~ 10 Hz readout rate. Faster rates are also possible by integrating over less than one line cycle at the expense of measurement resolution (~ 1 pA baseline for 0.1 cycles integration).

Three stripline beam position monitors along the line will measure the centroid position. Each strip has a length of ~ 14.5 cm and maximum sensitivity around 500 MHz. Simulated circuit response of in-house readout boards to a signal equivalent to 500 pC/30 ps beam already showed resolution on the order of $15 \mu\text{m}$ at 125MHz. For smaller charges, down to 10 pC/0.5 ps, simulations show noisy signals, still detectable with a resolution on the $100 \mu\text{m}$ scale. Those boards are now being adapted changing the working frequency from 125MHz to 260MHz, almost doubling the sensitivity.

Transverse Parameters Measurements

The emittance measurement system makes use of the 1D pepper pot method. The beam is cut by a series of two slits in the same direction (either vertical or horizontal), and the remaining charge is detected at the Faraday cup. The first slit selects the space coordinate (x or y), while the second, at a distance of 40 cm, selects the angle (x' or y'). Two couples of fast correctors (~ 100 Hz) before each collimator are used to scan the beam on the slits, mapping the trace space. The system has been designed to handle the beam full power (750 W at 1 mA). A first copper-made water-cooled armor slit $200 \mu\text{m}$ width absorbs more than 90% of beam power. Next, a $10 \mu\text{m}$ width tungsten slit thermally isolated from the previous one select the beamlet to be measured. The second collimator does not need an armor, since the current is already low. Coupling fast correctors with the VME QDC module, make it possible to scan the trace space at 100 Hz, and have a complete measurement in ~ 1 s, (on a 10×10 sampling).

Imaging screens are used for transverse shape measurements. Two different materials are planned to be used: Ce:Yag scintillators and BeO ceramics. Ce:Yag scintillation screens $100 \mu\text{m}$ thick have a good resolution and a high photon yield (10^4 photons per MeV deposited). A thin aluminum layer creates a path for electrons, preventing voltage build up in the insulating material. BeO have much worst resolution, but higher saturation threshold, and

will be used as back up option. An interlock of 10W on the beam power has been foreseen for insertion diagnostics such as screens and Faraday cup. Such power level does not seem to be a limiting factor: screens here will mostly be used for laser alignment on the cathode, thermal emittance measurements and solenoid related studies.

Longitudinal Measurements

The last section of the beamline is dedicated to longitudinal and slice properties measurements. Typical bunch lengths of the order of tens of picosecond are expected out of the rf gun. Those beams will require high compression factors to reach the high current needed by FEL for efficient performances, and the compression efficiency may be severely limited by longitudinal phase space distortions at low energies. Another important parameter for FEL performances is the slice energy spread, and values below 1 keV are expected out of the gun.

To perform such measurements we plan to install a one cell deflecting cavity at 1.3 GHz (Fig1). The low beam energy allow the use of TWT to supply RF power to the structure in CW mode. Blue and red curves left plot of Fig.2 shows time and energy resolution for a 750 keV beam versus the cavity input power, for a transverse shunt impedance of 5 MΩ. Formulas for angular kick and induced energy spread from deflecting structures can be found in [9]. In the measure of longitudinal phase space the Panowsky-Wenzel theorem [10] links the time resolution to the energy resolution. We derived a formula for the longitudinal emittance resolution as function of beam parameters. In the case of a drift between the RFD and the screen, with a beam waist at the screen position:

$$\left(\frac{\sigma_E^{ind}}{m_0 c^2}\right) \cdot (c\sigma_\tau^{ris}) = \varepsilon_y^n \sqrt{1 + \frac{L^2}{\beta_{y,0}^2}} \quad (1)$$

Where L is the distance between the deflector and the screen, β_0 is the beta function at the screen, ε_y^n is the normalized emittance in the deflection plane. It is clear that the longitudinal phase space resolution does not depend from the deflecting voltage (green curve in left plot of Fig.2), which increases the time resolution but also the induced energy spread. The resolution would be maximized for a 1:1 imaging optics from the RF deflector to the screen. This would be equivalent of $L = 0$ in Eq.1. In the case of a drift, for $\beta_{y,0}=L=1\text{m}$ we lose a factor $\sqrt{2}$. For a fixed L , a tighter focus on the screen will actually worsen the resolution (decrease of $\beta_{y,0}$), since this would lead to higher beam sizes and divergences at the deflector position. The only parameter that can increase the resolution is the beam emittance. In right graph of Fig.2 we report the resolution dependence on the transverse emittance. A vertical collimator can be placed right before the cavity to cut charge and decrease the emittance itself. A factor of 10 would bring the emittance below $0.1 \mu\text{m}$.

A dipole magnet after the deflecting cavity creates a dispersive region and deviates the electron beam toward a

Sources and Medium Energy Accelerators

Accel/Storage Rings 08: Linear Accelerators

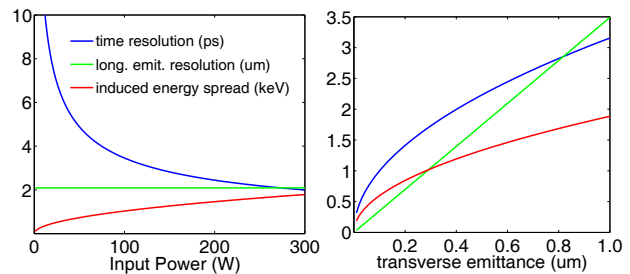


Figure 2: Time and Energy resolution dependence from rf deflector input power (left) and beam emittance (right). The transverse emittance used is $0.6 \mu\text{m}$.

screen 0.5 meters downstream. The magnet we plan to use has a bending angle $\alpha=\pi/2$ and a magnetic length of 0.54 m. A magnetic field on-axis of 112 G is needed for a 750 keV electron beam. The energy resolution can be derived by equalizing the intrinsic angle spread of the beam with the chromatic angle spread of the magnet. In the case of a drift with a beam waist at the screen we have:

$$\sigma_E^{res} = \frac{\gamma}{\sqrt{4\gamma^2 - 1}} \frac{m_e c^2}{\alpha} \cdot \sqrt{\frac{\varepsilon_x^n}{\beta_{x,0}}} \quad (2)$$

where γ is the Lorentz factor, $m_e c^2$ is the electron rest energy, ε_x^n is the normalized emittance in the dispersion plane, and $\beta_{x,0}$ is the Twiss parameter at the screen. We assume a beam waist at the screen and no focussing optics between the magnet and the screen. For a beam with $\varepsilon_x^n = 0.6 \mu\text{m}$ we get an energy resolution of 500 eV. Also in this case an emittance decrease would improve the resolution (a factor 10 in emittance is ~ 3 in energy resolution).

With a two-dimension scraper (round collimator or a double cross slit system) longitudinal measurements can be greatly improved, and the system resolutions would allow us to discriminate different contributions to the slice energy spread.

REFERENCES

- [1] J. Corlett *et al.*, this Conference.
- [2] K. Baptiste *et al.*, NIM A **599**, 9 (2009).
- [3] I.V. Bazarov *et al.*, Phys. Rev. ST Accel. Beams **11**, 100703 (2008).
- [4] S. Belomestnykh, V. Shemelin *et al.*, in the Proceedings of PAC'07, Albuquerque, p. 2331-2333.
- [5] <http://www.bergoz.com/>.
- [6] Cremat CR-11X-INST and CR-200-XX-INST, <http://www.cremat.com>.
- [7] CAEN V965A, www.caen.it.
- [8] Keithley Model 6487, <http://www.keithley.com>.
- [9] S. Korepanov *et al.*, in the Proceedings of DIPAC'07, Venice, Italy, p. 144-146.
- [10] T. Wangler, "Principles of RF Linear Accelerators", Edited by Wiley Interscience, 1998.